

Solution Multi-NMR and Raman Spectroscopic Studies of Thermodynamically Unstable XeO₄. The First ¹³¹Xe NMR Study of a Chemically Bound Xenon Species[†]

Michael Gerken and Gary J. Schrobilgen*

Department of Chemistry, McMaster University, Hamilton, Ontario L8S 4M1, Canada

Received June 12, 2001

Xenon tetroxide is thermodynamically unstable, decomposing explosively in the gas phase and in the solid state. A modified and more detailed description of the procedure for the preparation of XeO₄ and its solutions is provided. Xenon tetroxide dissolves in SO₂ClF, BrF₅, and HF solvents, giving solutions that are kinetically stable up to –30 °C. The preparation of kinetically stable XeO₄ solutions lays the groundwork for the solution chemistry of XeO₄ and for the extension of the presently limited chemistry of xenon(VIII). The ¹²⁹Xe and ¹⁷O NMR spectra of XeO₄ were observed for the first time, and the tetrahedral symmetry of XeO₄ allowed for the observation of a surprisingly narrow ¹³¹Xe resonance, the first ¹³¹Xe NMR study of a xenon compound. A variable temperature and variable field strength study of the spin–lattice relaxation times for ¹²⁹Xe and ¹³¹Xe show that the spin-rotation and the quadrupolar relaxation mechanisms, respectively, are dominant. The Raman spectrum of XeO₄ in anhydrous HF solvent confirms the absence of significant solvent–solute interactions.

Introduction

Xenon forms two binary oxides, XeO₃ and XeO₄, which are a solid and a gas, respectively, at room temperature. Both are thermodynamically unstable compounds that decompose explosively into their elements with the release of 402¹ and 642 kJ mol^{–1},² respectively. Despite their hazardous natures, structural data have been obtained from a single-crystal X-ray diffraction study of XeO₃,³ and an electron diffraction study of gaseous XeO₄.⁴ Vibrational frequencies for XeO₄ have been obtained in the gas phase by infrared spectroscopy⁵ and in the solid state by Raman spectroscopy.⁶

Xenon possesses two spin-active isotopes, ¹²⁹Xe (*I* = 1/2, 26.4% natural abundance) and ¹³¹Xe (*I* = 3/2, 21.1% natural abundance), but only ¹²⁹Xe is widely used for the structural characterization of xenon compounds.^{7–9} Until now, NMR

studies of ¹³¹Xe have been limited to elemental xenon.¹⁰ Although the natural abundance of ¹³¹Xe is similar to that of ¹²⁹Xe and the receptivity of ¹³¹Xe is high (0.104 relative to ¹²⁹Xe),¹¹ the quadrupolar nature of ¹³¹Xe causes fast spin–lattice relaxation in asymmetric environments had precluded any reports of ¹³¹Xe chemical shifts for chemically bound xenon. Xenon-131 chemical shifts and spin–lattice relaxation times have been determined for liquid and solid xenon, and the solvent dependencies of ¹³¹Xe chemical shift and *T*₁ values have been investigated for ¹³¹Xe in a number of solvents.¹⁰

Ruthenium, osmium, and xenon are the only elements in the periodic table to display the highest attainable oxidation state, +8. In recent years, considerable progress has been made in extending and understanding the fundamental oxide fluoride chemistry of osmium(VIII).^{12–15} This chemistry is

[†] Dedicated to Professor Pekka Pyykkö on the occasion of his 60th birthday.

* To whom correspondence should be addressed. E-mail: SCHROBIL@McMASTER.CA.

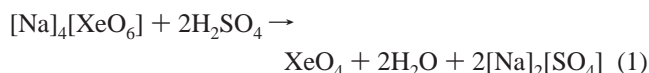
- (1) Gunn, S. R. In *Noble Gas Compounds*; Hyman, H. H., Ed.; The University of Chicago Press: Chicago, IL, 1963; pp 149–151.
- (2) Gunn, S. R. *J. Am. Chem. Soc.* **1965**, *87*, 2290.
- (3) Templeton, D. H.; Zalkin, A.; Forrester, J. D.; Williamson, S. M. *J. Am. Chem. Soc.* **1963**, *85*, 817.
- (4) Gunderson, G.; Hedberg, K.; Huston, J. L. *J. Chem. Phys.* **1970**, *52*, 812.
- (5) Selig, H.; Claassen, H. H.; Chernick, C. L.; Malm, J. G.; Huston, J. L. *Science* **1964**, *143*, 1322.
- (6) Huston, J. L.; Claassen, H. H. *J. Chem. Phys.* **1970**, *52*, 5646.

- (7) Gerken, M.; Schrobilgen, G. J. *Coord. Chem. Rev.* **2000**, *197*, 335.
- (8) Ratcliffe, C. I. *Annu. Rep. NMR Spectrosc.* **1998**, *36*, 123.
- (9) Schrobilgen, G. J. In *The Encyclopedia of Nuclear Magnetic Resonance*; Grant, D. M., Harris, R. K., Eds.; John Wiley and Sons: New York, 1996; pp 3251–3262.
- (10) Luhmer, M.; Reisse, J. *Prog. Nucl. Magn. Reson. Spectrosc.* **1998**, *33*, 57.
- (11) Mason, J. *Multinuclear NMR*; Plenum Press: New York, 1987; Appendix, p 625.
- (12) Christe, K. O.; Dixon, D. A.; Mack, H. G.; Oberhammer, H.; Pagelot, A.; Sanders, J. C. P.; Schrobilgen, G. J. *J. Am. Chem. Soc.* **1993**, *115*, 11279.

wholly reliant upon OsO₄, the synthetic precursor for all osmium(VIII) compounds. In contrast, the treacherous nature of XeO₄ has no doubt impeded progress in xenon(VIII) chemistry, which has progressed little beyond the synthesis and structural characterization of the remarkably stable perxenate anion, XeO₆⁴⁻,^{16–19} and the work by Huston and co-workers, who first synthesized^{5,20} and structurally characterized^{4–6} XeO₄. Huston and co-workers also demonstrated the existence of the only other xenon(VIII) compounds XeO₃F₂,²¹ which they characterized by matrix-isolation infrared spectroscopy, and XeO₂F₄,²² which has only been characterized in the gas phase by mass spectrometry. Both oxide fluorides were derived from XeO₄ by oxygen–fluorine metathesis with XeF₆. The goals of the present study were to characterize XeO₄ in solution for the first time and to establish protocols for safely creating synthetically useful XeO₄ solutions which have sufficient kinetic stability to further extend the little studied chemistry of xenon(VIII).

Results and Discussion

Preparation of XeO₄ Solutions. Although XeO₄ is highly explosive in the solid and gaseous states, XeO₄ solutions have been prepared for the first time which are kinetically stable at low temperatures. Xenon tetroxide was prepared from [Na]₄[XeO₆] and 100% sulfuric acid according to eq 1



and is based on a modification of the method of Huston et al.,⁵ which used concentrated sulfuric acid.

Solution samples of XeO₄ studied in this work were prepared by condensing XeO₄ into an FEP trap using the apparatus depicted in Figure 1 (for details, see the Experimental Section), followed by slow condensation of the appropriate solvent above the XeO₄ layer and slow melting of the solvent onto frozen XeO₄ while maintaining the resulting SO₂ClF and HF solutions at –78 °C and BrF₅ solutions at approximately –55 °C. Solutions of XeO₄ in SO₂ClF, HF, and BrF₅ were found to be stable at temperatures below –30 °C, at which temperature slow decomposition commenced. At 0 °C, decomposition rates in solution were rapid, but not explosive.

Characterization of XeO₄ by ¹²⁹Xe NMR Spectroscopy. The preparation of SO₂ClF, BrF₅, and HF solutions of XeO₄

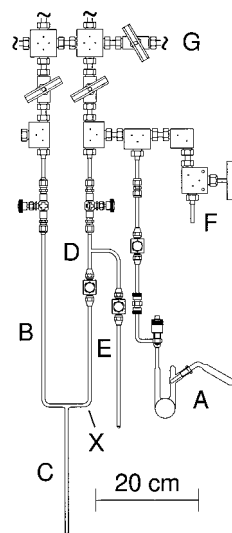
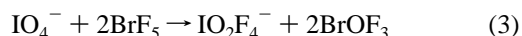
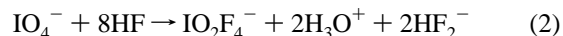


Figure 1. Apparatus for the generation of XeO₄ in HF and BrF₅ solvents: (A) glass vessel with rotatable side arm joined to a Kel-F valve by means of 1/4-in. o.d. × 1/8-in. i.d. FEP tubing and a 1/4-in. 316 stainless steel Cajon Ultra-Torr union, and to the metal vacuum line by means of a 1/4-in. nickel tube connection and 1/4-in. PTFE Swagelok union; (B) 1/4-in. o.d. FEP U-tube equipped with two Whitey ORF2 stainless steel valves; (C) 1/4-in. FEP sample tube; (D) FEP T-piece; (E) 1/4-in. o.d. FEP HF/BrF₅ solvent storage vessel equipped with a Kel-F valve; (F) 1/4-in. nickel tube connection for SO₂ClF solvent storage vessel; (G) metal vacuum line manifold constructed from 3/8-in. × 1/8-in. nickel tube connectors and from 316 Autoclave Engineers Inc. valves (30VM6071), crosses (CX-6666), T-pieces (CT-6660), and elbows (CL-6600); (X) condensation point for XeO₄ at –196 °C.

has provided the first NMR spectroscopic characterization of XeO₄. The ¹²⁹Xe chemical shifts of XeO₄ in SO₂ClF (–80 °C), BrF₅ (–50 °C), and HF (–75 °C) solutions are –92.9, –94.7, and –85.5 ppm, respectively (Figure 2 and Table 1). The chemical shift differences are very small when compared with those of other xenon species, e.g., XeF₂ (δ(¹²⁹Xe) = –1905 ppm in SO₂ClF, 25 °C; –1592 ppm in HF, 25 °C),²³ indicating that the tetrahedral molecule interacts only weakly with its solvent environment (see Characterization of XeO₄ by ¹³¹Xe NMR Spectroscopy). The small differences are likely attributable to differences in the bulk susceptibilities of the solvents. The temperature dependence of the ¹²⁹Xe chemical shift of XeO₄ was studied in SO₂ClF solvent up to 0 °C, where decomposition became rapid. The chemical shifts and the corresponding temperatures are listed in Table 2 and were found to increase slightly with increasing temperature.

Only XeO₄ was observed by ¹²⁹Xe NMR spectroscopy in HF and BrF₅ solutions, indicating that XeO₄ is not solvolyzed in either HF or BrF₅, which is in agreement with the Raman spectroscopic characterization of XeO₄ in HF solvent (see Raman Spectroscopic Characterization of XeO₄ in HF Solvent), but contrasts with the solvolytic behavior of the isoelectronic IO₄[–] anion in anhydrous HF solvent (eqs 2 and 3).²⁴



(23) Schrobilgen, G. J.; Holloway, J. H.; Granger, P.; Brevard, C. *Inorg. Chem.* **1978**, *17*, 980.

- (13) Casteel, W. J., Jr.; Dixon, D. A.; Mercier, H. P. A.; Schrobilgen, G. *J. Inorg. Chem.* **1996**, *35*, 43.
 (14) Gerken, M.; Dixon, D. A.; Schrobilgen, G. *J. Inorg. Chem.* **2000**, *39*, 4244.
 (15) Gerken, M.; Dixon, D. A.; Schrobilgen, G. *J. Inorg. Chem.* **2002**, *41*, 259.
 (16) Malm, J. G.; Holt, B. D.; Bane, R. W. In *Noble Gas Compounds*; Hyman, H. H., Ed.; University of Chicago Press: Chicago, IL, 1963; p 167.
 (17) Appleman, E. H.; Malm, J. G. *J. Am. Chem. Soc.* **1964**, *86*, 2141.
 (18) Ibers, J. A.; Hamilton, W.; MacKenzie, D. R. *Inorg. Chem.* **1964**, *10*, 1412.
 (19) Zalkin, A.; Forrester, J. D.; Templeton, D. H. *Inorg. Chem.* **1964**, *10*, 1417.
 (20) Huston, J. L.; Studier, M. H.; Sloth, E. N. *Science* **1964**, *143*, 1161.
 (21) Claassen, H. H.; Huston, J. L. *J. Chem. Phys.* **1971**, *55*, 1505.
 (22) Huston, J. L. *Inorg. Nucl. Chem. Lett.* **1968**, *4*, 29.

Table 1. ^{129}Xe and ^{131}Xe NMR Parameters for XeO_4

$\delta(^{129}\text{XeO}_4)_{\text{XeOF}_4}$, ppm ^a	$\Xi(^{131}\text{XeO}_4)$, Hz	$\delta(^{131}\text{XeO}_4)_{\text{Xe, Freon 114}}$, ppm ^b	$\delta(^{131}\text{XeO}_4)_{\text{XeOF}_4}$, ppm ^c	$\Delta\nu_{1/2}(^{131}\text{Xe})$, Hz	solvent	T , °C
-92.9	8 243 147	5195.6	-92.8	18	SO_2ClF	-78.5
-85.8	8 243 205	5202.7	-85.8	30	HF	-75
-94.7	8 243 133	5193.9	-94.5	96	BrF_5	-50

^a Chemical shifts are referenced to liquid XeOF_4 at 30 °C. ^b Chemical shifts are referenced to xenon gas dissolved in Freon 114 at 30 °C. ^c Chemical shifts are referenced to the hypothetical ^{131}Xe resonance of liquid XeOF_4 at 30 °C and were arrived at using eq 11.

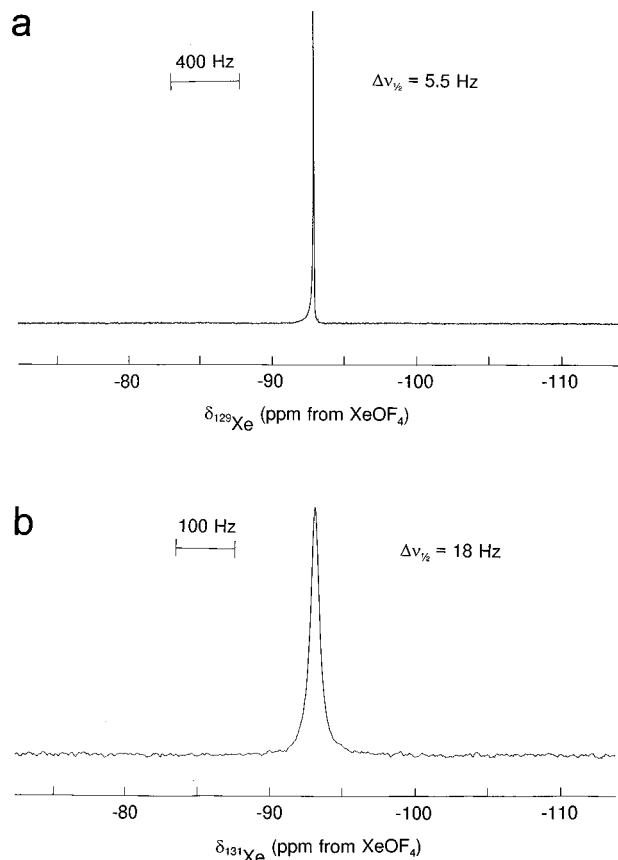


Figure 2. Xenon NMR spectra of XeO_4 in SO_2ClF solvent: (a) ^{129}Xe NMR spectrum (82.981 MHz) at -78.5 °C and (b) ^{131}Xe NMR spectrum (24.598 MHz) at -76 °C.

Table 2. Temperature Dependence of the ^{129}Xe Chemical Shift and ^{131}Xe Absolute Frequency of XeO_4 in SO_2ClF

T , °C	$\delta(^{129}\text{XeO}_4)$, ppm	$\Xi(^{131}\text{XeO}_4)$, Hz
-42	-90.0	8 243 172
-50	-90.8	8 243 163
-60	-91.6	8 243 158
-70	-92.5	8 243 150
-78.5	-92.9	8 243 148

The chemical shift ranges reported for ^{129}Xe in different oxidation states are very large,^{7–9} and the ^{129}Xe environments of $\text{Xe}(\text{VIII})$ compounds are expected to be less shielded than those of $\text{Xe}(\text{VI})$ compounds.²⁵ It is therefore surprising, at first glance, that ^{129}Xe in XeO_4 is significantly more shielded (-92.9 ppm for XeO_4 in SO_2ClF at -80 °C) than in XeO_3 (217 ppm for XeO_3 in H_2O at room temperature).²⁶ The low-

frequency chemical shift of XeO_4 can be accounted for using the formulation of Jameson and Gutowsky²⁷ for the paramagnetic contribution to the chemical shift, which normally dominates the chemical shifts of heavy nuclei. The paramagnetic shielding term under this formalism is given by eq 4, where Δ is the average excitation energy, $\langle 1/r^3 \rangle_p$ and

$$\sigma^p = -\left(\frac{2e^2\hbar^2}{3\Delta m^2 c^2}\right)\left(\left\langle\frac{1}{r^3}\right\rangle_p P_u + \left\langle\frac{1}{r^3}\right\rangle_d D_u\right) \quad (4)$$

$\langle 1/r^3 \rangle_d$ are the expectation values for $1/r^3$, r is the radius of the valence p and d orbitals, respectively, and P_u and D_u represent the “imbalance” of the valence electrons in the respective p and d orbitals centered on the atom in question. Calculations on a small number of xenon species have shown that a localized description of the bonding employing d hybridization provides a more satisfactory description than a delocalized description without d hybridization.²⁷ Moreover, the approach showed that Δ , $\langle 1/r^3 \rangle_{5p}$, and $\langle 1/r^3 \rangle_{5d}$ can be regarded as essentially constant over the range of xenon compounds considered so that P_u and D_u determine variations in $\delta(^{129}\text{Xe})$. For spherically symmetric closed shell atoms, P_u and D_u have their minimum values of zero and, in the tetrahedral XeO_4 molecule, P_u and D_u are close to zero, resulting in a small paramagnetic contribution to the xenon chemical shift, i.e., higher shielding of the xenon nucleus.

Characterization of XeO_4 by ^{17}O NMR Spectroscopy.

The ^{17}O NMR spectrum of natural abundance XeO_4 in $\text{SO}_2\text{-ClF}$ was recorded at -78 °C. Besides the solvent signal at $\delta = 226$ ppm ($\Delta\nu_{1/2} = 80$ Hz), a weak signal at 509 ppm ($\Delta\nu_{1/2} = 46$ Hz) was observed. The $^1J(^{129}\text{Xe}-^{17}\text{O})$ coupling was not observed because of the broadness of the signal. The line width of the ^{17}O resonance is largely a consequence of the quadrupolar nature of the ^{17}O nucleus ($I = 5/2$, natural abundance = 0.037%) and the relatively high viscosity of SO_2ClF at -78 °C, which serves to increase the rotational correlation time, τ_c , leading to increases in both the rate of quadrupolar relaxation and the line width. The ^{17}O chemical shift for XeO_4 complements the series of known chemical shift values for tetrahedral MO_4^{n-} species in which M is in the highest possible oxidation state (Table 3). The ^{17}O chemical shift of XeO_4 follows the previously noted trend for tetrahedral MO_4^{n-} molecules²⁸ in which ^{17}O becomes more deshielded as the atomic number of M increases within a period, paralleling the electronegativity order within the period. With an ^{17}O chemical shift of 509 ppm, the oxygens of XeO_4 are significantly more deshielded than those of the

(24) Christie, K. O.; Wilson, R. D.; Schack, C. J. *Inorg. Chem.* **1981**, *20*, 2104.

(25) Jameson, C. J. In *Multinuclear NMR*; Mason, J., Ed.; Plenum Press: New York, 1987; Chapter 3, pp 66–68.

(26) Seppelt, K.; Rupp, H. H. *Z. Anorg. Allg. Chem.* **1974**, *409*, 331.

(27) Jameson, C. J.; Gutowsky, H. S. *J. Chem. Phys.* **1964**, *40*, 1714.

(28) Dove, M. F. A.; Sanders, J. C. P.; Appelman, E. H. *Magn. Reson. Chem.* **1995**, *33*, 44.

Table 3. Oxygen-17 Chemical Shifts (ppm) of Main Group and Transition Metal Element Tetraoxo Species^a

group							
5	6	7	8	15	16	17	18
				PO ₄ ³⁻	SO ₄ ²⁻	ClO ₄ ⁻	
				99	167	292	
VO ₄ ³⁻	CrO ₄ ²⁻	MnO ₄ ⁻	—	AsO ₄ ³⁻	SeO ₄ ²⁻	BrO ₄ ⁻	
568	835	1230		108	204	360	
—	MoO ₄ ²⁻	TcO ₄ ⁻	RuO ₄	—	—	IO ₄ ⁻	XeO ₄
	831	748	1106			243	509
—	WO ₄ ²⁻	ReO ₄ ⁻	OsO ₄				
	420	569	796				

^a With the exception of XeO₄, all ¹⁷O chemical shifts are taken from ref 28 and references therein.

isoelectronic IO₄⁻ (243 ppm) anion, representing the most deshielded ¹⁷O environment for a main group MO₄ⁿ⁻ species encountered thus far. The trend is consistent with the higher electronegativity of Xe(VIII) relative to that of I(VII). The ¹⁷O chemical shift of XeO₄ is, however, significantly more shielded than those of the neutral transition metal tetroxides, OsO₄ and RuO₄, and, with the exception of WO₄²⁻, the transition metal tetraoxo anions (Table 3). The ¹⁷O chemical shift of XeO₃ in H₂O (278 ppm)²⁹ is significantly more shielded than the ¹⁷O resonance of XeO₄. The relative deshielding of the XeO₄ ¹⁷O chemical shift is evidence for the greater electronegativity of Xe(VIII) relative to that Xe(VI). In comparison, the ¹⁷O chemical shifts of the halates follow the same trends as those of the perchlorates, but the differences between the ¹⁷O chemical shifts of ClO₄⁻, BrO₄⁻, and IO₄⁻ (Table 3) and those of ClO₃⁻ (287 ppm),²⁹ BrO₃⁻ (297 ppm),³⁰ and IO₃⁻ (206 ppm),³¹ while consistent with the greater electronegativity of the halogen in the +7 oxidation state than in the +5 oxidation state, are substantially less than between XeO₄ and XeO₃.

Characterization of XeO₄ by ¹³¹Xe NMR Spectroscopy.

Besides ¹²⁹Xe, ¹³¹Xe is the only other naturally occurring xenon isotope (21.4% natural abundance) that is NMR active. It is, however, quadrupolar ($I = 3/2$), providing a very efficient relaxation pathway by means of interaction of the quadrupolar moment with an electric field gradient (efg). The rate of quadrupolar relaxation under conditions of extreme narrowing is given by eq 5, where $\Delta\nu_{1/2}$ is the line width at

$$\Delta\nu_{1/2} = \frac{1}{\pi T_1^Q} = \frac{1}{\pi T_2^Q} = \frac{3\pi}{10} \left(\frac{2I+3}{I^2(2I-1)} \right) \left(1 + \frac{\eta^2}{3} \right) \left(\frac{e^2 Q q}{h} \right)^2 \tau_c \quad (5)$$

half-height, T_1^Q the spin–lattice relaxation time, T_2^Q the spin–spin relaxation time, I the nuclear spin quantum number, η the asymmetry parameter, Q the quadrupole moment, q the electric field gradient, e the electronic charge, and τ_c the isotropic rotational correlation time. The rotational

correlation time, as defined by Noggle and Schirmer,³² is related to the rotational diffusion constant, D_r , by

$$\tau_c = \frac{1}{6D_r} \quad (6)$$

where

$$D_r = \frac{\langle \Delta\theta^2 \rangle}{2t} \quad (7)$$

and $\langle \Delta\theta^2 \rangle$ is the net mean-squared angle turned in time t . The rotational correlation time is approximated for spherical solute and solvent molecules by the Stokes–Einstein equation (eq 8) and is a function of temperature, T , effective

$$\tau_c = \frac{\eta V_m f_r}{kT} \quad (8)$$

volume of the solute molecule, V_m , the viscosity of the solvent, η , and f_r , the microviscosity factor. Quadrupolar relaxation often leads to broadening of the NMR resonance of the quadrupolar nuclide to the extent that it is indistinguishable from the spectral baseline as is the case for the majority of ¹³¹Xe compounds. The line width factor, WF (eq 9), which is characteristic for a specific quadrupolar nucleus,

$$WF = Q^2 \left(\frac{2I+3}{I^2(2I-1)} \right) \quad (9)$$

gives an indication of the size of the interaction between the nuclear quadrupole moment and the efg. Until now, the width factor of ¹³¹Xe ($19 \times 10^{-59} \text{ m}^4$)¹¹ only permitted the observation of ¹³¹Xe NMR signals from xenon gas.^{8,10} In the present study, the high symmetry of XeO₄ (T_d point symmetry) has made possible the observation of the first ¹³¹Xe NMR chemical shift of chemically bound xenon (Figure 2).

Direct referencing of the ¹³¹Xe chemical shift of XeO₄ to the accepted standard for ¹²⁹Xe NMR spectroscopy, liquid XeOF₄,⁹ is not possible because the ¹³¹Xe resonance of XeOF₄ is broadened to such an extent by quadrupolar relaxation (vide supra) that it is rendered indistinguishable from the spectral baseline. Referencing of the ¹³¹Xe resonance of XeO₄ to that of XeOF₄ was indirectly achieved using the procedure outlined by Jameson³³ and is represented by eq 10, where δ_1 is the ¹³¹Xe chemical shift of XeO₄ relative to

$$\delta_1 = \delta_2 \left(\frac{\nu_{\text{ref}2}}{\nu_{\text{ref}1}} \right) + \delta_{\text{ref}2, \text{ref}1} \quad (10)$$

the primary reference, liquid XeOF₄; δ_2 is the ¹³¹Xe chemical shift relative to the secondary reference, xenon gas dissolved in Freon 114 solvent; $\nu_{\text{ref}1}$ and $\nu_{\text{ref}2}$ are the absolute frequencies, $\Xi(^{131}\text{XeOF}_4)$ and $\Xi(^{131}\text{Xe}, \text{Freon } 114)$, respectively; and $\delta_{\text{ref}2, \text{ref}1}$ is the ¹³¹Xe chemical shift of the secondary

(29) Reuben, J.; Samuel, D.; Selig, H.; Shamir, J. *Proc. Chem. Soc., London* **1963**, 270.

(30) Figgis, B. N.; Kidd, R. G.; Nyholm, R. S. *Proc. R. Soc. London, Ser. A* **1962**, 269, 269.

(31) Dwek, R. A.; Luz, Z.; Peller, S.; Shporer, M. *J. Am. Chem. Soc.* **1971**, 93, 77.

(32) Noggle, J. H.; Schirmer, R. E. *The Nuclear Overhauser Effect: Chemical Applications*; Academic Press: New York, 1971; pp 26–31.

(33) Jameson, C. J. In *Nuclear Magnetic Resonance, Specialist Periodical Reports*; Webb, G. A., Ed.; The Royal Society of Chemistry: Cambridge, 1998; Vol. 27, p 44.

reference with respect to the primary reference. Ignoring the primary isotope effect, which is expected to be negligible, $\delta_{\text{ref2,ref1}}$ can be measured in the ^{129}Xe spectrum and is the chemical shift of xenon gas dissolved in Freon 114 with respect to XeOF_4 ($\delta(^{129}\text{Xe}, \text{Freon 114})_{\text{XeOF}_4} = -5261.6$ ppm). The value for the absolute frequency of the primary reference, $\Xi(^{131}\text{XeOF}_4)$, can be approximated by that of XeO_4 , $\Xi(^{131}\text{XeO}_4)$. The absolute ^{131}Xe frequencies of XeO_4 and xenon gas dissolved in Freon 114 are referenced to the ^1H NMR signal of TMS at exactly 100 MHz. The absolute ^{131}Xe frequency determined for xenon gas dissolved in Freon 114 at 30 °C was 8 200 540 Hz, and those determined for XeO_4 in SO_2ClF , HF, and BrF_5 solvents are listed in Table 1. Substitution of the appropriate terms into eq 10 yields the expression (eq 11) for the ^{131}Xe chemical shift of XeO_4 with respect to the hypothetical ^{131}Xe NMR resonance of XeOF_4 .

$$\delta(^{131}\text{XeO}_4)_{\text{XeOF}_4} = \frac{\delta(^{131}\text{XeO}_4)_{\text{Xe, Freon 114}} \Xi(^{131}\text{Xe}, \text{Freon 114})}{\Xi(^{131}\text{XeO}_4)} + \delta(^{129}\text{Xe}, \text{Freon 114})_{\text{XeOF}_4} \quad (11)$$

The ^{131}Xe chemical shifts that are arrived at using eq 11 are in excellent agreement with the ^{129}Xe chemical shifts, providing unambiguous proof for the assignment of the ^{129}Xe and ^{131}Xe resonances to tetrahedral XeO_4 .

The line width of the ^{131}Xe resonance is surprisingly narrow (Table 1). Nuclei with comparable width factors like ^{71}Ga and ^{209}Bi ($\text{WF} = 16 \times 10^{-59} \text{ m}^4$ and $10 \times 10^{-59} \text{ m}^4$,²⁹ respectively) exhibit larger line widths in highly symmetric environments at room temperature. Line widths of 100 Hz have been observed for aqueous solutions of GaX_4^- ($\text{X} = \text{Cl}, \text{Br}, \text{I}$),³⁴ and the line width of the ^{209}Bi signal of BiF_6^- in acetone at room temperature was found to be 44 Hz.³⁵ Unlike XeO_4 , the anionic natures of these tetrahedral and octahedral species result in ion pairing in solution, possibly causing distortion of the symmetry and an increase in the effective volume and in τ_c (eq 8), resulting in broader NMR signals. The narrow ^{131}Xe line widths obtained for XeO_4 indicate the absence of any significant interactions between XeO_4 and the solvents studied. Such interactions would result in distortion of XeO_4 from T_d symmetry, leading to more rapid quadrupolar relaxation of the ^{131}Xe nucleus and significant broadening of the ^{131}Xe NMR signal. This serves to confirm the inertness of XeO_4 toward solvolytic attack and the absence of strong solvation interactions with HF, BrF_5 , and SO_2ClF , which are corroborated by ^{129}Xe NMR spectroscopic studies. The reluctance of XeO_4 to expand its coordination number in the solvents studied in the present work is likely a consequence of the steric demand of four large $\text{Xe}=\text{O}$ double bond domains.

Spin–Lattice (T_1) Relaxation of the ^{129}Xe and ^{131}Xe Nuclei in XeO_4 . Spin–lattice relaxation rates for the ^{129}Xe

Table 4. Spin–Lattice (T_1) Values for XeO_4 in SO_2ClF Solution at Variable Temperature and External Field Strength

T , °C	$T_1(^{129}\text{Xe})$, ms ^a	$T_1(^{131}\text{Xe})$, ms ^a
−42	423	46.1
−50	444	40.3
−61	554	36.2
−70	701 (743)	29.6 (29.4)
−76	801	26.7
−79	(834)	(24.9)

^a Spin–lattice relaxation times were determined at external magnetic field strengths of 7.0463 or 11.744 T (values in parentheses).

and ^{131}Xe nuclei in XeO_4 dissolved in SO_2ClF were studied at variable temperatures and at two different magnetic field strengths using standard inversion–recovery experiments. The T_1 -relaxation times, their corresponding temperatures, and field strengths are listed in Table 4.

Several relaxation mechanisms can contribute to the observed total spin–lattice relaxation time (T_1), namely, the nuclear dipole–dipole interaction (T_1^{DD}), the chemical shift anisotropy mechanism (T_1^{CSA}), the nuclear quadrupole interaction (T_1^{Q}), scalar coupling (T_1^{SC}), the spin-rotation mechanism (T_1^{SR}) and interaction with paramagnetic species, (T_1^{E}). Under conditions of extreme narrowing, the very strong quadrupolar interaction normally dominates the spin–lattice relaxation time for quadrupolar nuclei. Because the molecular correlation time decreases with increasing temperature (eq 8), the still very efficient T_1^{Q} process becomes less effective in inducing spin–lattice relaxation so that T_1 also decreases with increasing temperature (eq 5), as was found for ^{131}Xe in XeO_4 (Table 4). For some low Q nuclei such as ^9Be ($I = 3/2$, $Q = 0.0529 \times 10^{-28} \text{ m}^2$)³⁶ in $[\text{Be}(\text{H}_2\text{O})_4]^{2+}$, it was found that the spin-rotation mechanism becomes the dominant relaxation pathway at higher temperatures, i.e., > 50 °C.³⁷ This results in a maximum in a plot of T_1 versus T because T_1^{SR} follows an inverse temperature dependence. This behavior was not observed for ^{131}Xe in XeO_4 because the quadrupole moment of ^{131}Xe ($Q = -0.114 \times 10^{-28} \text{ m}^2$)³⁸ is significantly larger than that of ^9Be and it is not possible to increase the temperature sufficiently because of the instability of XeO_4 at higher temperatures.

The inverse temperature dependence of $T_1(^{129}\text{Xe})$ in XeO_4 indicates that the spin-rotation relaxation is the dominant relaxation pathway. The spin-rotation mechanism is the only spin–lattice relaxation mechanism that exhibits a decrease in T_1 with increasing temperature. As expected for the highly symmetric XeO_4 molecule, the CSA relaxation mechanism was not found to play a significant role in the total spin–lattice relaxation time because no significant differences in T_1 values were found for ^{129}Xe and ^{131}Xe when measured at two different field strengths (7.0464 and 11.744 T). Seppelt and Rupp³⁹ reported ^{129}Xe T_1 values for several xenon compounds assuming a dominant dipole–dipole mechanism. A thorough study of the spin–lattice relaxation rates for ^{129}Xe in XeF_2 has been reported by Jokisaari et al.,⁴⁰ which

(36) Pyykkö, P. *Mol. Phys.* **2001**, *99*, 1617.

(37) Wehrli, F. J. *Magn. Reson.* **1978**, *30*, 193.

(38) Kellö, V.; Pyykkö, P.; Sadlej, A. J. *Chem. Phys. Lett.* **2001**, *346*, 155.

(39) Seppelt, K.; Rupp, H. H. *Z. Anorg. Allg. Chem.* **1974**, *409*, 338.

(34) Akitt, J. W.; Greenwood, N. N.; Storr, A. *J. Chem. Soc.* **1965**, 4410.

(35) Morgan, K.; Sayer, B. G.; Schrobilgen, G. J. *J. Magn. Reson.* **1983**, *52*, 139.

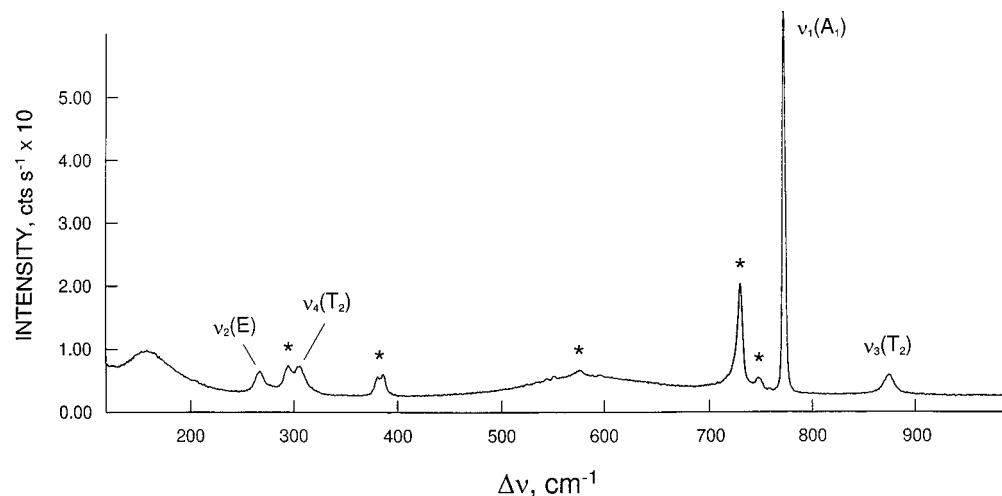


Figure 3. Raman spectrum of an HF solution of XeO₄ recorded in FEP at $-74\text{ }^{\circ}\text{C}$ using 514.5-nm excitation. Asterisks (*) denote FEP sample tube lines.

Table 5. Vibrational Frequencies and Their Assignments for Solid and Gaseous XeO₄ and for a Solution of XeO₄ in HF

frequencies, ^a cm ⁻¹			
XeO _{4(s)} ^b -195 °C	XeO _{4(g)} ^{b,c} RT	XeO ₄ in HF solvent ^d -74 °C	assignment XeO ₄ (T _d)
875.9	877 ^c	878 (5.5)	$\nu_3(\text{T}_2)$
867.0			
860.5			
767.1	773	776 (100)	$\nu_1(\text{A}_1)$
311.5	305.7 ^e	305 (7.5)	$\nu_4(\text{T}_2)$
301.8			
295.7			
280.0	n.o.	267 (5.5)	$\nu_2(\text{E})$
273.6		156 (7)	unassigned

^a Values in parentheses denote relative Raman intensities; abbreviations: denote not observed (n.o.); room temperature (RT). Frequencies were obtained from the Raman spectrum if not indicated otherwise. ^b Reference 5. ^c Reference 6. ^d Bands arising from the FEP sample tube were observed at 294 (8), 381 (5), 386 (6), 578 (1), 733 (27), and 750 (3). ^e Band observed in the infrared spectrum of XeO_{4(g)}, ref 5.

demonstrated that the dipole–dipole mechanism is negligible. The T_1 versus T plot showed a maximum indicating that the CSA mechanism was dominant at low temperatures and that the spin-rotation mechanism was dominant at high temperatures. No maximum in the T_1 versus T plot could be found for ¹²⁹Xe in XeO₄. Because only spin-dilute nuclei are present in XeO₄, the nuclear dipole–dipole relaxation mechanism is not expected to make a significant contribution to T_1 .

Raman Spectroscopic Characterization of XeO₄ in HF Solvent. The Raman spectrum of XeO₄ in HF solvent was recorded at $-74\text{ }^{\circ}\text{C}$ (Figure 3), and the observed frequencies, listed in Table 5, are compared with those of gaseous^{5,6} and solid XeO₄.⁶ The solution spectrum resembles that of XeO₄ in the gas phase (differences $\leq 3\text{ cm}^{-1}$), indicating that the structure of XeO₄ in HF solvent is that of the undistorted tetrahedral molecule found in the gas phase which is in accord with the ¹³¹Xe NMR spectroscopic findings (see Characterization of XeO₄ by ¹³¹Xe NMR Spectroscopy).

Conclusions

A more detailed procedure for the synthesis of XeO₄ has been reported which, for the first time, provides for the preparation of solution samples of XeO₄. Xenon tetroxide has been stabilized in several oxidatively resistant and synthetically useful solvent media and characterized in these solutions by ¹²⁹Xe, ¹³¹Xe, and ¹⁷O NMR and Raman spectroscopy. The highly symmetric environment around xenon in XeO₄ gives rise to surprisingly narrow ¹³¹Xe NMR resonances, the first reported ¹³¹Xe NMR resonances of chemically bound xenon. The temperature dependencies of the ¹²⁹Xe and ¹³¹Xe spin–lattice relaxation times established the dominance of the spin-rotation relaxation and quadrupolar relaxation mechanisms, respectively. The kinetic stabilities of the XeO₄ solutions studied in the present work lay the groundwork for the investigation of the solution chemistry of xenon in the +8 oxidation state. These studies will be presented in future publications.

Experimental Section

CAUTION! Anhydrous HF and BrF₅ must be handled using appropriate protective gear with immediate access to proper treatment procedures in the event of contact with liquids, their vapors, or their solutions. Bromine pentafluoride reacts explosively with organic materials; therefore, the use of organic cooling baths should be avoided. Xenon tetroxide is explosive in the solid state, and the dissolution of XeO₄ in the solvents, SO₂ClF, HF, and BrF₅, must be treated with great caution, because explosions can occur when cold solvent is initially brought into contact with solid XeO₄ at temperatures close to $-196\text{ }^{\circ}\text{C}$ (see Preparation of XeO₄ Solutions). In the present work, small quantities of XeO₄ (50 mmol and under) in approximately 0.5 mL of HF, BrF₅, or SO₂ClF solvents were disposed of by slowly pouring the cold solution (0 °C or lower) into several liters of a mixture of ice and aqueous NaOH inside a properly shielded fume hood. Solution sample containers must be handled with long metal tongs and protective gloves when dumping their contents into the disposal medium. *It is not advisable to use the above procedure for the disposal of significantly larger quantities of XeO₄ or BrF₅.*

Manipulations involving volatile materials were performed under strictly anhydrous conditions on a vacuum line constructed from 316 stainless steel, nickel, Teflon, and FEP, and nonvolatile

(40) Ingman, L. P.; Jokisaari, J.; Oikarinen, K.; Seydoux, R. *J. Magn. Reson., Ser. A*, **1994**, *111*, 155.

materials were handled in the atmosphere of a drybox as previously described.⁴¹ The solvents HF,⁴² SO₂ClF,²³ and BrF₅⁴² were purified using standard literature methods. Sodium perxenate was prepared according to the method of Jaselskis et al.⁴³ and Appelman et al.⁴⁴ by hydrolysis of XeF₆ followed by ozonization of the basified solution using carbonate-free NaOH. Xenon hexafluoride was prepared as described previously.⁴⁵

Preparation of XeO₄ Solutions. The procedure for the preparation of XeO₄ is a modification of the procedure first reported by Huston, Studier, and Sloth.²⁰ Solutions of XeO₄ were prepared using an apparatus depicted in Figure 1. A glass vessel (A) which was equipped with a 4-mm Teflon/glass stopcock (J. Young Scientific) and a rotatable glass side arm containing [Na]₄[XeO₆] was used for the generation of XeO₄. The vessel was connected to a metal submanifold through a 20-cm length of 1/4-in. o.d. FEP tubing. One side of a 1/4-in. o.d. FEP U-trap (B), equipped with two stainless steel valves (Whitey ORF2), was directly attached to the submanifold of the metal vacuum line. The other side of the FEP U-tube was connected to the metal submanifold through a Kel-F valve attached to a 1/4-in. o.d. FEP T-piece (D) which was, in turn, connected to the submanifold through a stainless steel valve (Whitey ORF2). The side arm of the 1/4-in. FEP T-piece was bent and attached to a 1/4-in. o.d. FEP tube fitted to a Kel-F valve (E), which was used for corrosive solvents (HF and BrF₅). A graduated glass vessel equipped with a 6-mm Teflon/glass stopcock (J. Young Scientific) was used for containment of SO₂ClF when the latter solvent was employed. The latter vessel was connected to the metal submanifold at F through a fine metering valve (Monel Nupro model M-4MG-KZ-VH) in order to better control the rate at which SO₂ClF was condensed into U-tube B. A 1/4-in. o.d. FEP tube (C), heat fused to the bottom of the U-tube (B), served to contain the XeO₄ solution (vide infra and Figure 1).

In a typical experiment, a solution of XeO₄ was prepared by slow addition of 0.13 g (0.41 mmol) of [Na]₄[XeO₆] to ca. 16 mL of a 1:1 (v/v) mixture of concentrated sulfuric acid (British Drug Houses, 95–98%) and oleum (Baker Analyzed Reagents, free SO₃ 11–17%) at 0 °C with simultaneous condensation of XeO₄ under dynamic vacuum into a 1/4-in. o.d. FEP U-tube (B) at point X. A stainless steel dewar was used for containment of liquid nitrogen in the event of an explosion. Approximately 0.5 mL of solvent was slowly condensed at –196 °C at approximately a point ca. 15 cm above the frozen XeO₄ in one branch of the U-tube (point X in Figure 1). The solvent was subsequently allowed to slowly melt under static vacuum and flow down onto the frozen XeO₄, washing it into the terminal 1/4-in. o.d. FEP tube (C). This resulted in clear pale yellow solutions when the samples were warmed to the temperatures used to record their NMR spectra (Tables 1 and 4). (**CAUTION:** In several instances, melting solvents too rapidly onto XeO₄ held at –196 °C resulted in violent detonations because of thermal and/or pressure shock.) The terminal 1/4-in. o.d. FEP tube was heat-sealed off from the U-tube and used for NMR spectroscopic characterization by inserting the tube into an 8-mm o.d.

precision thin wall glass NMR tube which was, in turn, positioned with Teflon shims inside a 10-mm o.d. precision thin wall glass NMR tube.

Nuclear Magnetic Resonance Spectroscopy. Nuclear magnetic resonance spectra were recorded unlocked (field drift < 0.1 Hz h⁻¹) on Bruker AC-300 (7.0464 T) and DRX-500 (11.744 T) spectrometers equipped with an Aspect 3000 computer and a Silicon Graphics workstation, respectively. The ¹²⁹Xe and ¹³¹Xe spectra were obtained on the AC-300 spectrometer using a 10-mm broad band probe tuned to 82.981 and 24.598 MHz, respectively. The ¹⁷O spectrum was obtained on the DRX-500 spectrometer using a 10-mm broad band probe tuned to 67.784 MHz. Free induction decays were accumulated in 16K (32K) and 8K memories with spectral width settings of 20 (20 kHz) and 30 kHz, yielding acquisition times of 0.410 (0.410) and 0.136 s for ¹²⁹Xe (¹³¹Xe) and ¹⁷O, respectively. The number of transients accumulated for ¹²⁹Xe (¹³¹Xe) and ¹⁷O spectra were typically 5000 (2000) and 48 600 using pulse widths of 14 (30) and 15.7 μs, respectively; no relaxation delays were applied. The free induction decays were processed in 32 (32K) and 16K memories to give data point resolutions of 1.22 (1.22) and 1.83 Hz/data point; a line broadening of 1 (3) Hz was applied. The ¹²⁹Xe and ¹⁷O spectra were referenced to external samples of neat XeOF₄ and H₂O, respectively. The ¹³¹Xe spectra of XeO₄ and xenon gas dissolved in Freon 114 were initially referenced at 30 °C to the ¹H NMR signal of neat TMS at exactly 100 MHz, giving the absolute ¹³¹Xe frequencies of the ¹³¹Xe signal. The chemical shift convention used is that a positive (negative) sign signifies a chemical shift to high (low) frequency of the reference compound.

Measurements of the spin–lattice relaxation times T₁(¹²⁹Xe) and T₁(¹³¹Xe) of XeO₄ in SO₂ClF at variable temperatures were performed on a Bruker AC-300 [DRX-500] spectrometer using a 10-mm broad band probe and a standard inversion–recovery experiment (pulse sequence: π–τ–π/2–acquisition). A total of 50 [15/30] and 200 [50] scans were accumulated for each ¹²⁹Xe and ¹³¹Xe NMR spectrum, respectively, which were acquired using spectral widths of 20 kHz [¹²⁹Xe, 10 kHz; ¹³¹Xe, 20 kHz] and a 16 [16]K memory. The free induction decays were processed using a line broadening of 20 [2] Hz. A total of 10 to 14 [16] τ values were measured including τ_∞ = 5 [8 and 5] s and 300 [300] ms for ¹²⁹Xe and ¹³¹Xe, respectively. The T₁ values were obtained by iterative exponential fitting of the intensity values versus τ using standard Bruker software.

Raman Spectroscopy. The low-temperature Raman spectrum of XeO₄ in HF solvent at –74 °C was recorded on a Jobin-Yvon Mole S-3000 triple spectrograph system using the 514.5-nm line of an Ar⁺ ion laser as previously described.⁴¹

Acknowledgment. We thank the donors of the Petroleum Research Fund, administered by the American Chemical Society, for support of this work under Grant ACS-PRF No. 28284-AC3. We also thank the Ontario Ministry of Education and the Richard Fuller and James A. Morrison Memorial Funds for the award of graduate scholarships to M.G. and the Canada Council for the award of a Killam Research Fellowship (1998 and 1999) to G.J.S.

- (41) Casteel, W. J., Jr.; Kolb, P.; LeBlond, N.; Mercier, H. P. A.; Schrobilgen, G. J. *Inorg. Chem.* **1996**, *35*, 929.
 (42) Emara, A. A. A.; Schrobilgen, G. J. *Inorg. Chem.* **1992**, *31*, 1323.
 (43) Jaselskis, B.; Splittler, T. M.; Huston, J. L. *J. Am. Chem. Soc.* **1966**, *88*, 2149.
 (44) Appelman, E. H.; Williamson, S. M. *Inorg. Synth.* **1968**, *11*, 210.
 (45) Chernick, C. L.; Malm, J. G. *Inorg. Synth.* **1966**, *8*, 259.

IC010627Y